



Preparation of Pickering Emulsions Stabilized by Metal Organic Frameworks using Oscillatory Woven Metal Micro-Screen

Journal:	<i>Soft Matter</i>
Manuscript ID:	SM-ART-04-2015-000922.R1
Article Type:	Paper
Date Submitted by the Author:	28-Apr-2015
Complete List of Authors:	Sabouni, Rana; American University of Sharjah, Chemical engineering Gomaa, Hassan; Western University, Chemical and Biochemical Engineering

Preparation of Pickering Emulsions Stabilized by Metal Organic Frameworks using Oscillatory Woven Metal Micro-Screen

R. Sabouni ^a and H.G. Gomaa ^b

Department of Chemical and Biochemical Engineering, Western University, Ontario, Canada N6A5B9
^a Present address: Department of Chemical Engineering, American University of Sharjah, Sharjah, UAE.

Abstract:

Uniform Pickering emulsions stabilized by metal organic frameworks (MOFs) MIL-101 and ZIF-8 nanoparticles (NP) were successfully prepared using oscillatory woven metal microscreen (WMMS) emulsification system in presence and absence of surfactants. The effects of operating and system parameters including frequency and amplitude of oscillation, type of nano-particle or/and surfactant on the droplet size and coefficient of variance of the prepared emulsions are investigated. The results showed that, both the hydrodynamics of the system and the hydrophobic/ hydrophilic nature of the NP influenced the interfacial properties of the oil-water interface during droplet formation and after detachment, which in turn affected the final droplet size and distribution. Comparison between measured and predicted droplet size by simple torque balance (TB) model is discussed.

Keywords: Emulsion, Metal organic frameworks (MOFs), nano-particles, Oscillatory motion, and parametric study.

^b Corresponding authors, H. G. Gomaa, Chemical and Biochemical Engineering Department Western University, London, Ontario, Canada, N6A 5B9, Email: Hgomaa@uwo.ca

INTRODUCTION

Emulsions stabilized by solid particles, also known as Pickering emulsions (PE), has recently gained significant interest in many applications including pharmaceuticals, food products, cosmetics, and fuel processing¹. They offer several advantages over conventional surfactant stabilized emulsions such as high stability attributed to an almost irreversible adsorption of the solid-particles to the droplets interface which prevent their coalescence^{2,3}. Another advantage is the potential for using benign solid-particles as stabilizer that could provide additional functionality and possibly avoid adverse effects that may be linked to using surfactants in cosmetics and pharmaceutical applications⁴. Furthermore, PE can also be used as a platform for preparation of advanced materials templates such as Janus colloids⁵, microspheres⁶, and composite microcapsules⁷.

Successful realization of the aforementioned benefits is strongly dependent on, first, the choice of the stabilizing particles and its characteristics and functional properties. Second, and similar to surfactant stabilized emulsions, is also greatly influenced by the emulsification technique and its effect on the final emulsion particle size and distributions.

From the stabilizing particles selection point, there are several reports in the literature related to using variety of materials for preparation of PE including metal oxides, cellulose, bacteria, latexes, and colloid silica, with the latter being the most commonly used⁸⁻¹¹. From an emulsification technique point, most of the reported methods were based on conventional techniques such as high-pressure homogenization, ultrasonic devices, and rotor–stator systems. Such techniques however suffer from low energy efficiencies, broad droplet size distribution, and significant temperature and shear rise that could possibly have negative impact on product functional properties. To overcome some of these limitations, membrane emulsification (ME) was proposed as an effective alternative¹²⁻¹⁴. Although there are number of reports related to use of the ME for preparation of conventional surfactant stabilized emulsions, limited information has been published on its application for preparation of PE.

The main objectives of this contribution is to first, explore the potential of using new material namely, metal organic frameworks (MOFs), as particle stabilizer for preparation of PE. MOFs are new class of crystalline nanoporous compounds that has gained significant interest recently for their attractive features in many applications including separation processes,

catalytic reactions, and anticancer drug delivery, and can potentially offer many opportunities for preparation of new materials based on PE¹⁵⁻¹⁷. The second objective of this research is to investigate the feasibility and process characteristics of preparing such emulsions using a novel oscillatory membrane emulsification technique based on the dynamic membrane emulsification (DME) principles¹⁸⁻²⁰. The design has the advantage of decoupling the continuous phase flow from the surface shear thus overcoming the relatively low dispersed phase concentrations limitation typically encountered in conventional cross flow membrane emulsification²¹⁻²⁸. Characterization of the prepared emulsions as well as the MOFs particles are presented. The effect of process parameters on particle size and distribution together with droplet formation mechanisms are discussed. The effect of combining both conventional surfactants and MOFs nanoparticles on the emulsions properties is also investigated, and the results of the measured droplet sizes are compared to theoretical modeling predictions.

EXPERIMENTAL

Materials

Two particular types of MOFs particles are investigated as emulsion stabilizer based on their reported excellent potential for applications such as drug loading and delivery. First is ZIF-8, which is a tetrahedrally connected framework of composition $Zn(2-MeIm)_2$ (2-MeIm = 2-methylimidazole) which belongs to the Zeolite Imidazolate Frameworks (Fig. 1a).

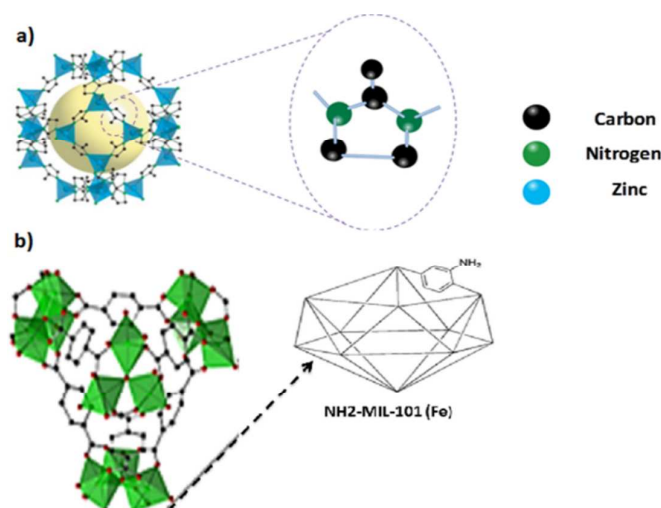


Figure 1. Crystal Structure of a) ZIF-8 and b) MIL-101^{29, 30}

It displays high water stability and flexible sorption behaviour¹⁷. The pores structure are accessed through ~ 0.3 nm windows, and exhibits strong hydrophobic nature¹⁸. It combines the characteristics of both MOFs (tuneable pore size and high surface area) and Zeolite (high stability in aqueous solutions), which makes it an excellent candidate for drug delivery applications³¹⁻³³. The second is Amine Materials of Institute of Lavoisier-101- Frameworks, NH₂-MIL-101 (Fe), or MIL-101, which is of the prototypical carboxylate-based MOFs that is composed of terephthalic acid linkers and Fe₃ salt, and has been recognized for its high drug loading and delivery capacities^{34,35} (Fig1b). It has larger accessible pore windows (~ 0.6 -1.0 nm), and is more hydrophilic than ZIF-8.

MIL-101 MOFs was prepared as shown before³⁶ by dissolving mixture of NH₂-terphthalic acid (organic linker) and of FeCl₃ (metal salt) in dimethylformamide (DMF) followed by microwave thermal treatment for period 30-90 seconds. The product was filtered and washed with DMF, then dried in a vacuum oven at 25 °C. ZIF-8 was purchased from Sigma-Aldrich and used without further purification.

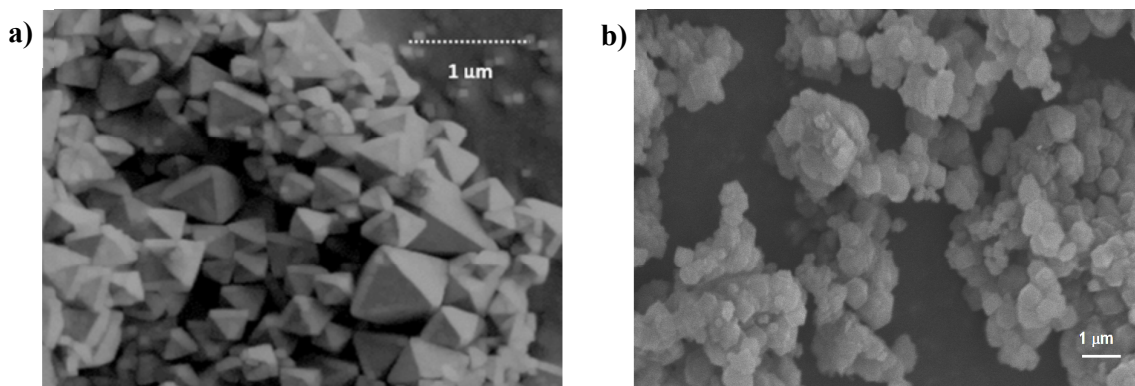


Figure 2. SEM of a) ZIF-8 and b) MIL-101

The particles were characterized using X-ray diffraction analysis (XRD) and scanning electron microscopy (SEM). The XRD was done at ambient temperature using Rigaku – MiniFlex powder diffractometer (Japan), and CuK α (λ for K α = 1.54059 Å) over 2θ range of 5° to 40° with step width of 0.02°. The SEM images were taken by Joel instrument (JSM 600F model, Japan) operating at 10 keV of acceleration voltage (Figs. 2a, b). Non-ionic surfactant Polyoxyethylene sorbitan monolaurate (Tween-20) obtained from Sigma-Aldrich was used for emulsions prepared with both surfactant and MOFs NP. The interfacial tensions

were measured using FTA1000 drop shape instrument, B system with FTA video drop shape software by First Ten Angstroms. The viscosities were measured using rheometer model LVDE115. The physical properties of the systems used are listed in Table 1.

Table 1: Physical Properties of the Systems

<u>Equilibrium interfacial tension (mN/m)</u>	
Oil-Water	26.716
ZIF-8 in water- Oil	0.381
ZIF-8 in oil-Water	0.401
Oil-NH ₂ -MIL-101(Fe) in water	5.783
Oil-NH ₂ -MIL-101(Fe) in water & 1% Tween 20 in water	3.436
<u>Viscosity (Pa.s)</u>	
Continuous phase (water)	0.0010
Continuous phase (ZIF-8 & Water)	0.0015
Continuous phase (ZIF-8 1% Tween 20 & Water)	0.0016
Continuous phase (NH ₂ -MIL-101(Fe) & Water)	0.0013
Continuous phase (NH ₂ -MIL-101(Fe) 1% Tween 20 & Water)	0.0014
Dispersed phase (oil)	0.55
Dispersed phase (ZIF-8 in oil)	0.50
<u>Density (kg/m³)</u>	
Continuous phase density (kg/m ³)	1000
Dispersed phase density (kg/m ³)	920
<u>NH₂- MIL-101(Fe) NP physical properties</u>	
Chemical formula	C ₆ H ₇ FeNO ₄
Particle size (μm)	0.2
Density (kg/m ³) ³⁷	620
HBL	both
<u>ZIF-8 physical properties</u>	
Chemical formula	C ₈ H ₁₀ N ₄ Zn
Particle size (μm)	0.5
Density (kg/m ³) ³⁸	1450
HBL ¹⁷	hydrophobic

Experimental Setup

The oscillatory woven metal micro-screen (WMMS) apparatus consists of 1.5L Plexiglas rectangular container filled with the continuous phase, and emulsification unit made of two 35 mm x 25 mm WMMS sheets housed in the sides of flat surface frame with tapered end. The WMMS is made of stainless steel plain weaves (38μm pore size and 36% porosity) in

which each weft wire passes alternately over and under each wrap wire and each wire passes alternately over and under each weft wire. The dispersed phase was injected through the microscreen by peristaltic pump (Pharmacia Fine Chemicals P-3 Peristaltic Pump) with variable speed motor to control the flow rate. The oscillations frequency was controlled by variable speed motor, while the amplitude was set using an eccentric system. This arrangement provided wide range of frequencies and amplitude ($f= 0-20$ Hz, and $a= 0-20$ mm). Fig. 3 shows a schematic representation of the experimental apparatus.

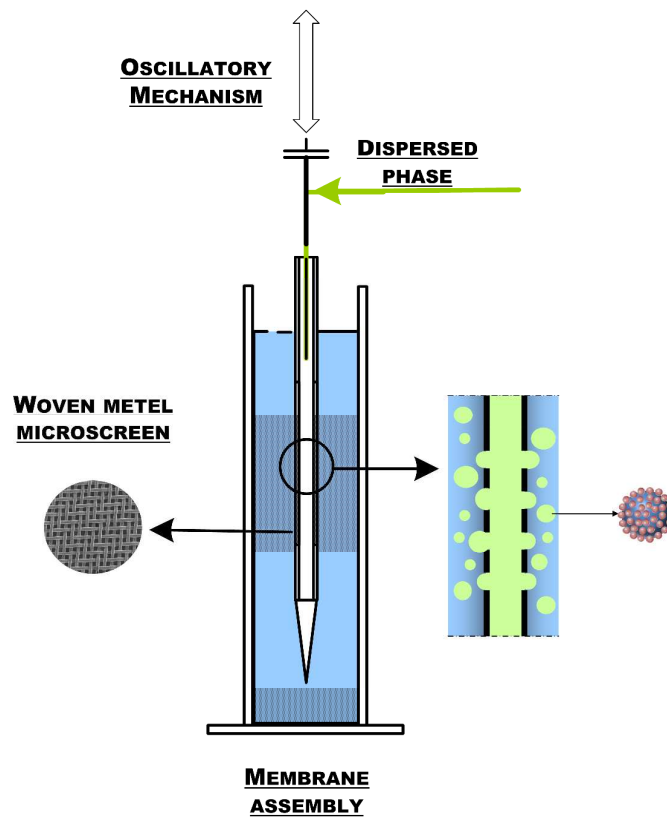


Figure 3. The Oscillatory woven metal-screen (WMMS) apparatus

Emulsion Preparation and Characterization

All emulsions were prepared by dispersing 12.5 mL commercial vegetable oil in 400 mL distilled water and 100 mg nanoparticles. The latter were stirred in distilled water for 15 minutes before each experiment to ensure homogenous distribution. For combined surfactant-nanoparticles (NP) stabilized emulsions, 1% of Tween 20 was added to the continuous aqueous phase together with the NP. At the end of each experiment, 100 ml of sample was

collected for emulsions droplets characterization. The apparatus was cleaned and rinsed thoroughly with distilled water after each experiment to eliminate any cross contamination.

Observation and characterization of emulsions were done using digital microscope (Ziess M2 1256 Microscope) and a video camera. The size distributions were estimated by image analysis. The average droplet size d was measured from 50-100 droplets immediately after each experiment. The droplet size distribution of each sample was measured using coefficient of variation (CV) for n droplets given as,

$$CV = \frac{1}{d} \sum_i^n \left[\frac{(d_i - d)^2}{n} \right]^{1/2} \quad (1)$$

RESULTS AND DISCUSSION

Figs. 4 shows typical microscopic image and droplet size distribution of the forming emulsions. In almost all cases, the droplet size distribution was essentially monomodal and Gaussian in appearance.

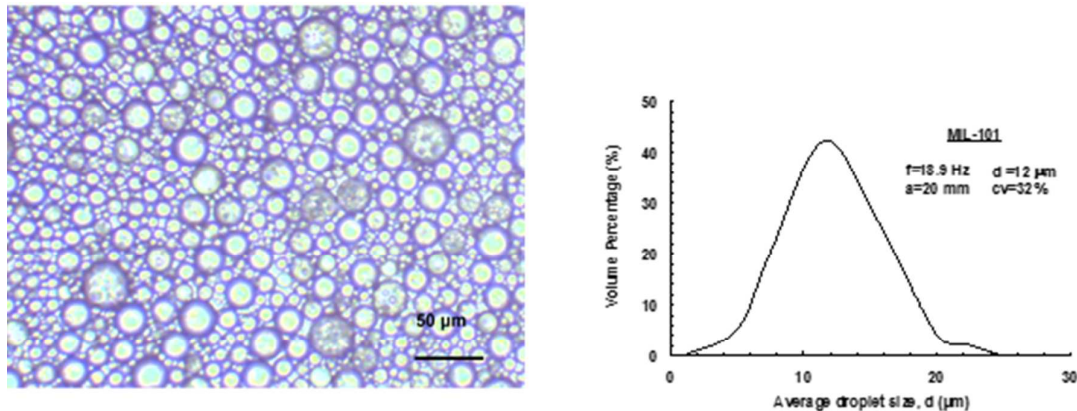


Figure 4. Microscopic image and droplet size distribution for emulsion prepared using MIL-101NPs

The produced emulsions had long shelf life with no evidence for droplets coalescence or ripening for over six months as shown in Fig 5. This clearly demonstrates the effectiveness of using MOFs as particle stabilizer for preparation of PE.

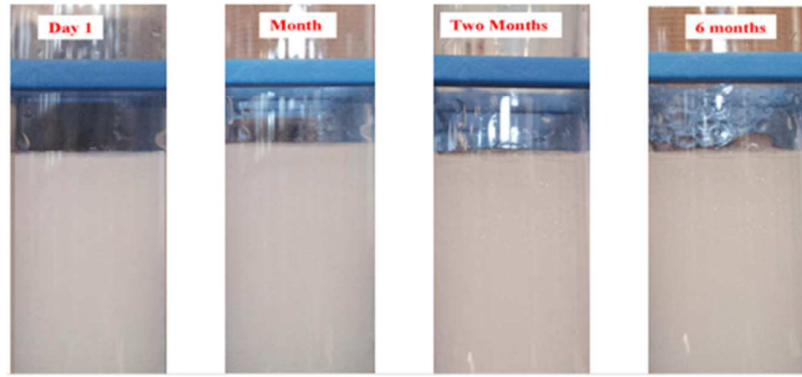


Figure 5. Stability of the formed emulsions over six months using ZIF-8 NPs ($f=18.9$ Hz, $a=6$ mm)

Effect of Nanoparticles (NPs)

The presence of NPs with affinity to the dispersed phase affects an emulsification process by their adsorption at the interface and the modification of the interfacial free energy due to the replacement of fluid-fluid with particle-fluid surface area. The reduction of the shared area between the phases creates a physical barrier to droplet coalescence, thus enhances the emulsion stability. If the free energy reduction due to particle adsorption is large compared to thermal and external forces due to for example shear stresses in the flow field, particles adsorption can become almost irreversible. In absence of NP, the thermodynamic state is,

$$\Delta E = A\gamma_o - NE_d \quad (2)$$

In which ΔE is the change in the total interfacial free energy, γ_o is the interfacial tension of the bare interface, N_p is the number of NPs in a given interfacial area A , and E_d is the desorption energy required to remove one NP from the interface given by,

$$E_d = \pi R^2 \gamma_o (1 - |\cos \theta|)^2 \quad (3)$$

Where R is the particle radius, and θ the particle contact angle. It can be seen that increasing the size of the NP leads to larger surface coverage and higher desorption energy, and therefore larger interfacial energy reductions. Previous investigations has also shown that NP-NP interactions can affect its configuration at the liquid-liquid interface, which in turn affects the surface pressure and interfacial energy³⁹. In this work, ZIF-8 and MIL-101 NPs were

used as emulsion stabilizer. The former has larger average particles size and higher hydrophobic nature than the latter. Such differences would be expected to result in stronger affinity of ZIF-8 NPs to the oil-water interface than MIL-101 NPs, and may possibly explain its stronger effect on droplet size and stability as will be discussed latter.

Effect of Oscillations on Droplet Size

In a drop- by- drop emulsification, droplet detachment occurs mainly when the shear caused by the drag force F_d created by the relative motion between the fluid and the surface exceeds the interfacial tension holding force F_s that keeps the droplet attached to the pore. For particle stabilised emulsions, and assuming particle adsorption is thermodynamically favoured; the kinetics for particle barrier formation must be matched to the drop-by-drop formation process to provide sufficient stability at the membrane surface to prevent coalescence. If the particle is weakly attached, which strongly depends on the particle affinity to the surface, it could diffuse away depending on the system characteristics and hydrodynamics.

Figs. 6a and 6b show the effect of oscillation frequency and amplitude on droplet size and distribution for emulsions prepared using ZIF-8. As can be seen, increasing the oscillation intensity decreases the emulsion droplet size as well as its polydispersity. This is due to the fact that, higher oscillation results in increasing the relative velocity between the fluid and the surface leading to increasing the drag force acting on the forming droplets. This in turn will lead to detachment of smaller droplet, and reduce the probability of its coalescence at the pores, as well as breakage after detachment.

The effect of the dispersed phase flux on droplets size is shown in Fig. 6c, which as can be seen, result in increasing the average droplet size. Such effect could be attributed to the droplet detachment process, which is not infinitely fast, but requires a certain time. During that time, the droplet volume increases with increasing the dispersed phase injection rate to values larger than the critical detachment size determined by force balance.

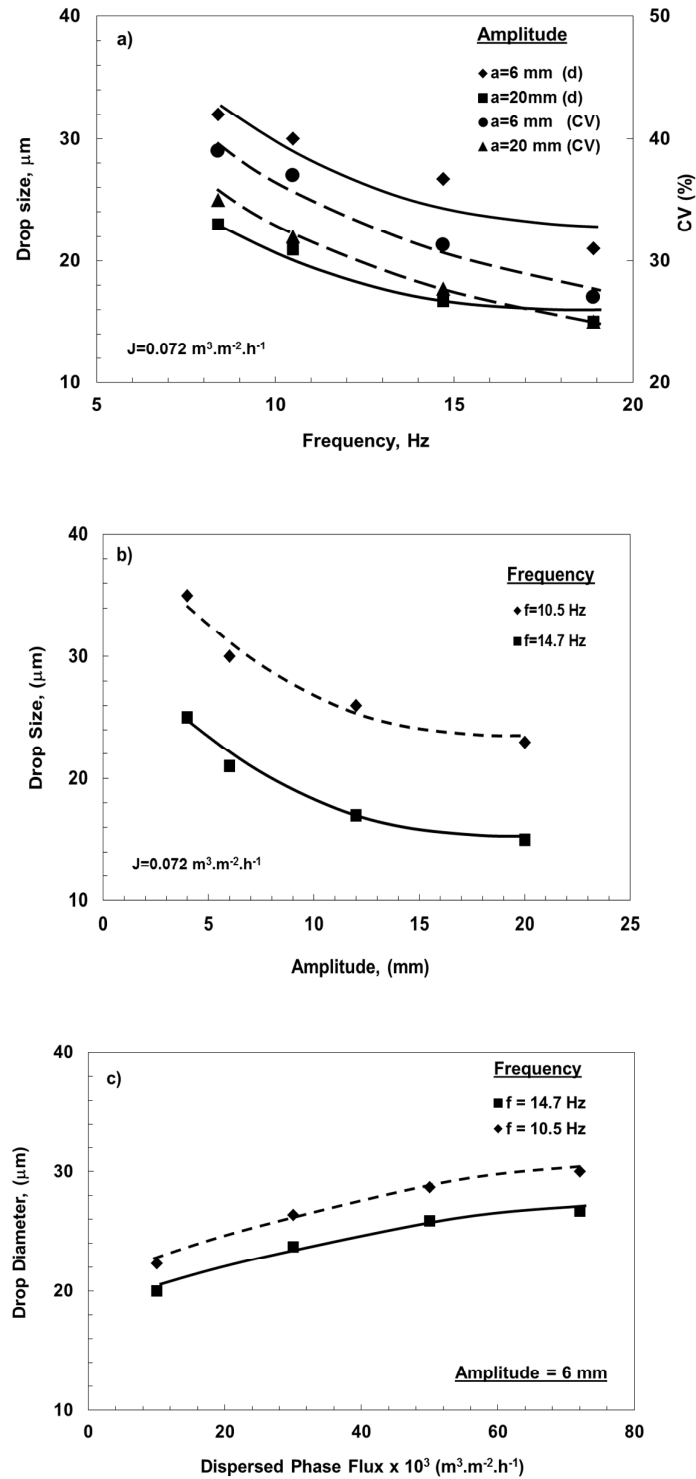


Figure 6. Variation of droplet size and distributions for emulsions stabilized using ZIF-8. Effect of: a) frequency, b) amplitude, c) dispersed phase flux.

To further investigate of whether the oscillations effect on particles diffusion towards the forming droplets may have contributed to the improved CV values, we conducted a set of experiments with ZIF-8 NPs dispersed in the oil phase as an emulsion stabilizer. Under such conditions, the NPs are readily available at the oil-water interface during droplet formation, thus eliminating the probability of diffusional limitation from the bulk to the interface during droplet formation if any.

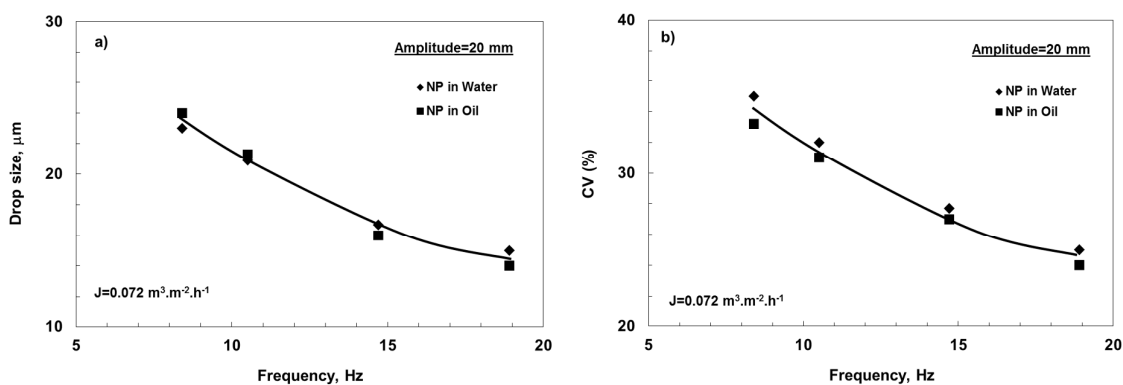


Figure 7. Comparison between emulsions prepared using ZIF-8 in oil and water. Effect of oscillation frequency on a) droplet size, b) size distribution (CV)

Figs. 7a and 7b show the change in droplets size and distribution with oscillation for these experiments together with results for emulsions prepared using ZIF-8 NPs dispersed in the continuous aqueous phase. It can be seen that there is hardly any difference between the two, which indicates that the convective flow field from the oscillatory motion provided sufficient particle flux to the growing droplet and that particle stabilization is not diffusion limited.

The effect of oscillations on the droplet size and distribution for emulsions produced using MIL-101 NPs are shown in Figs. 8a, and 8b, respectively. As can be seen, the general trend for the effect of frequency on droplet size and distribution is similar to that observed for emulsions stabilized with ZIF-8 NPs. The effect of amplitude on the emulsion uniformity however was opposite, where higher CV values were observed as the amplitude increased. Furthermore, comparison between MIL-101 and ZIF-8 results showed the latter to be more uniform (lower CV values), particularly at higher oscillations intensities. Such observations may suggest that the mechanisms affecting the final droplet size and distribution in one case may be different from those at work in the other.

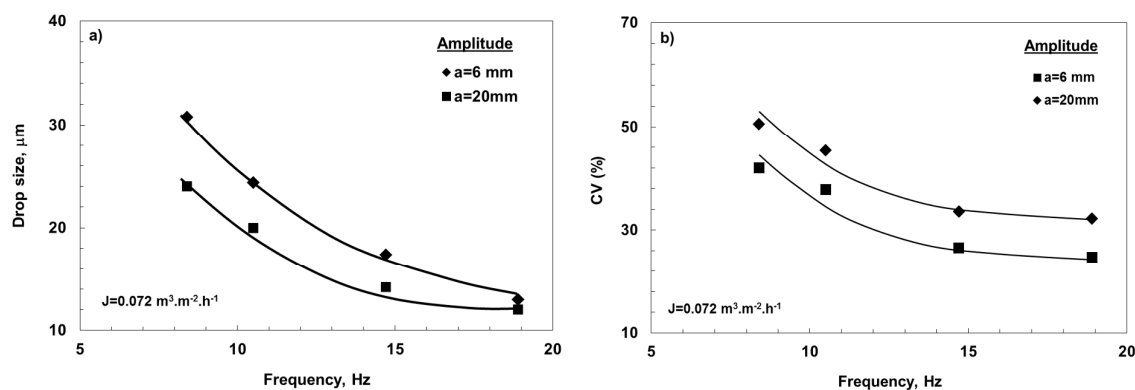


Figure 8. Characteristics of emulsions stabilized using MIL-101. Effect of oscillation frequency on: a) droplet size, b) size distribution (CV)

A possible explanation for such phenomena may be attributed to the fact that, NPs stabilize an emulsion if they remain strongly attached to the droplets surface, which varies depending on their binding force compared to other mobilization forces. The latter include thermal energy, which in most cases is much smaller than adsorption energy, leading to the commonly accepted argument of irreversible adsorption. Thermal energy however, may not be the only factor affecting NP attachment, since other forces related to the hydrodynamics of the system, such as shear stresses and flow eddies, could also play a nontrivial role in particle mobilization. This phenomenon can occur any time leading to particles removal from droplets surface and possible coalescence of the latter to larger sizes, which in turn can be fragmented due to shear stresses, or chaotic eddy structure during shear reversal in oscillatory flows. This may explain the observed results since the higher hydrophobic nature of ZIF-8 and its stronger affinity to the oil-water interface, could have resulted in formation of smaller and more stable droplets that resisted further breakage at higher oscillatory shear. MIL-101 on the other hand, and due to its less hydrophobic nature and possible lower droplet interface affinity, would be easier to detach from a droplet surface under the influence of the surrounding hydrodynamic forces leading to formation of larger droplets. Such droplets will have a higher tendency for breakage to smaller satellite ones, particularly at higher oscillation intensities leading to the broadening of the formed emulsion size distribution. Similar results have been reported previously when using high shear rates²⁸.

Effect of Combining Surfactant and Nanoparticles

Although there are valuable information in the literature on the interfacial properties of oil–water systems in presence of surfactant and NPs, particularly hydrophilic silica, the results suggest that the effect on the final emulsions properties depends strongly on the systems, the NP- surfactant interactions both at the droplet surface and in the bulk^{40,41}, as well as the preparation technique⁴²⁻⁴⁵. For example, surfactant adsorption on the NPs may result in particle agglomeration and adsorption of agglomerates at the oil/water interface leading to improved emulsion stability. On the other hand, surfactants which are bound onto the NP surface may not be as effective in lowering the interfacial tension compared to free ones. The energy gained by binding the surfactants onto a NP is countered by the entropic penalty of confining the surfactants onto the NP surface as well as the energy penalty of removing the surfactant from the oil–water interface to the NP. Increasing surfactant concentration could also result in displacing the NPs from the oil/water interface which may affect the emulsion droplet size and distribution⁴⁶. Furthermore, when particles decorated with various molecules are considered, particle-particle interactions could also have an effect on the interfacial energy³⁹. Figs. 9a, and 9b show representative results of oscillations effect of on droplet size and distribution for emulsions stabilised by Tween-20 surfactant and MIL-101 NPs as compared to emulsions prepared using NPs alone, under the same oscillatory conditions.

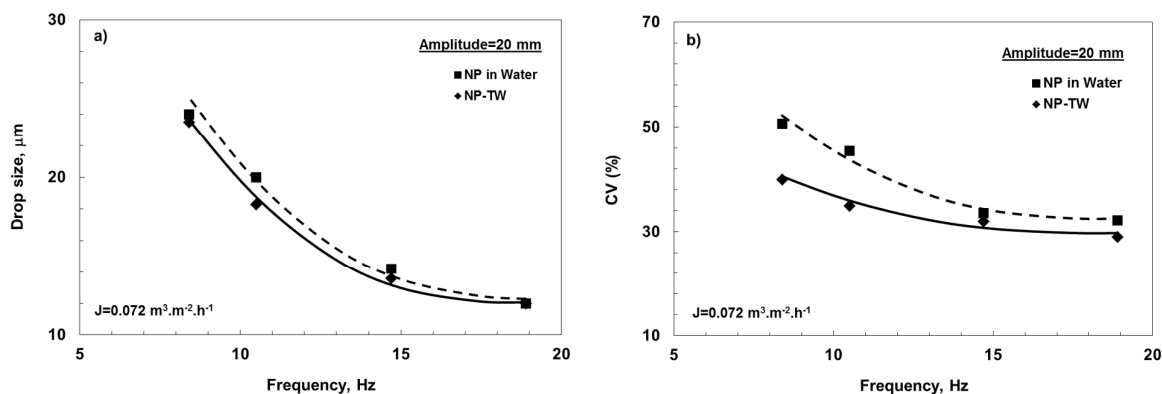


Figure 9. Emulsions stabilized with MIL-101 in presence of Tween-20 surfactant. Effect of oscillation frequency on a) droplet size, b) size distribution (CV)

As can be seen, the presence of surfactant did not significantly affect the average droplet size, but improved the distribution. This could possibly be attributed to a possible surfactant - NP

synergy in stabilizing the droplets and reducing its coalescence and/or breakage probability. Results for emulsions stabilized with Tween-20 and ZIF-8 NPs are shown in Figs 10a, 10b. Contrary to MIL-101, both larger droplet size and higher CV values are seen for ZIF-8. This may be explained by the possible NP interactions with the surfactant hydrophobic terminus which may have resulted in decreasing the affinity of both to the surface and consequently affecting droplet size and stability. This further support the assumption of surfactant interaction with both the liquid-liquid and the solid-liquid interfaces.

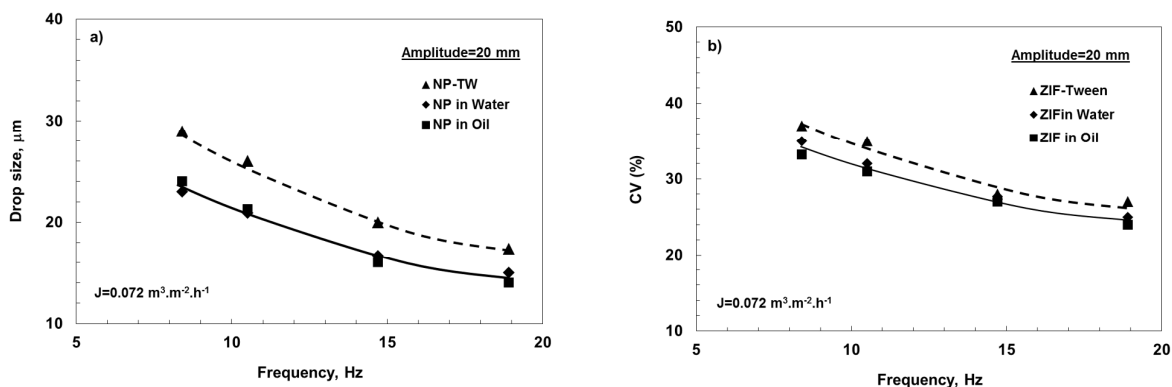


Figure 10. Emulsions stabilized with ZIF-8 in presence of Tween-20 surfactant. Effect of oscillation frequency on a) droplet size, b) size distribution (CV)

As discussed before, the effect of surfactant-NPs interaction on emulsion properties, which has been observed by previous investigators, may be explained based on the fact that, aside from a possible surfactant adsorption onto the NP which would limit its effectiveness, a surfactant may also displace NPs from the interface. This was confirmed by C. Vashisth, et.al.⁴⁶, who reported that application of shear resulted in displacing silica nanoparticles from the interface and the response of the latter to shear and deformation, changed with surfactant concentration as it continues to displace the nanoparticles. It was also reported that the displacement process is not instant, but spans over a time period during which larger droplets are formed that would then breakup to sizes comparable to those of droplets stabilized by the surfactant alone. In another investigation by Binks et. al.⁴⁷, it was found that stirring solutions of nonionic surfactant with particle-stabilised emulsions increased droplets coalescence as the surfactant adsorbed onto the particle surfaces and caused aggregation. Both of the mentioned investigations support the hypothesis of a possible change in emulsion size distribution due to surfactant interaction with NPs at the droplets surface, which could

lead to possible coalescence of the latter to larger size followed by fragmentation under the effect of shear and/ or flow eddies.

Comparison between Measured and Predicted Droplet Size

As mentioned earlier, droplet detachment in membrane emulsification occurs when the shear force F_d created by the relative motion between the fluid and the surface exceeds the interfacial tension holding force F_s . The latter is given by,

$$F_s = \pi d_p \gamma \quad (4)$$

For small droplets, the shear force acting on the droplet F_d may be approximated by,

$$F_d = (3/2)k_s \pi \tau d^2 \quad (5)$$

In the above equations, d_p is the pore diameter, and d the droplet diameter. The factor k_s is a wall correction factor, which for a sphere moving parallel to solid wall in a simple shear flow is $\sim 1.7^{48}$. For a surface oscillating harmonically with velocity $u_o = a\omega \cos \omega t$, in which a is the oscillation amplitude and ω the angular frequency, the velocity u of the fluid layer adjacent to the surface is given by the Stokes solution⁴⁹,

$$u = u_o e^{-\eta} \cos(\omega t - \eta) \quad (6)$$

From which, the maximum shear stress τ is,

$$\tau = a\omega^{3/2} (\rho_c \nu_c^{1/2}) \quad (7)$$

Where $\eta = y/\delta_s$, y , the distance from the surface, $\delta_s = \sqrt{2\nu_c/\omega}$, and ν_c and ρ_c are the continuous phase kinematic viscosity, and density, respectively. If the shape of the droplet can still be approximated by a sphere before detachment, and neglecting other forces such as static, lift, and buoyancy forces, the droplet diameter may be estimated from a torque balance (TB) between the drag and interfacial tension forces using⁵⁰,

$$F_d \sqrt{\left(\frac{d}{2}\right)^2 - \left(\frac{d_p}{2}\right)^2} = F_s \left(\frac{d_p}{2}\right) \quad (8)$$

Substituting for the drag and interfacial tension forces and solving gives,

$$d = \frac{\left[\tau^2 d_p^2 \left(\gamma + \sqrt{\gamma^2 - 3\tau^2 d_p^2} \right) \right]^{1/3}}{3^{2/3} \tau} + \frac{\tau d_p^2}{3^{1/3} \left[\tau^2 d_p^2 \left(\gamma + \sqrt{\gamma^2 - 3\tau^2 d_p^2} \right) \right]^{1/3}} \quad (9)$$

To simplify by assuming the drag force to act at the droplet centre, a torque balance becomes,

$$F_d \left(\frac{d}{2} \right) = F_s \left(\frac{d_p}{2} \right) \quad (10)$$

Substituting for the drag and interfacial tension forces gives,

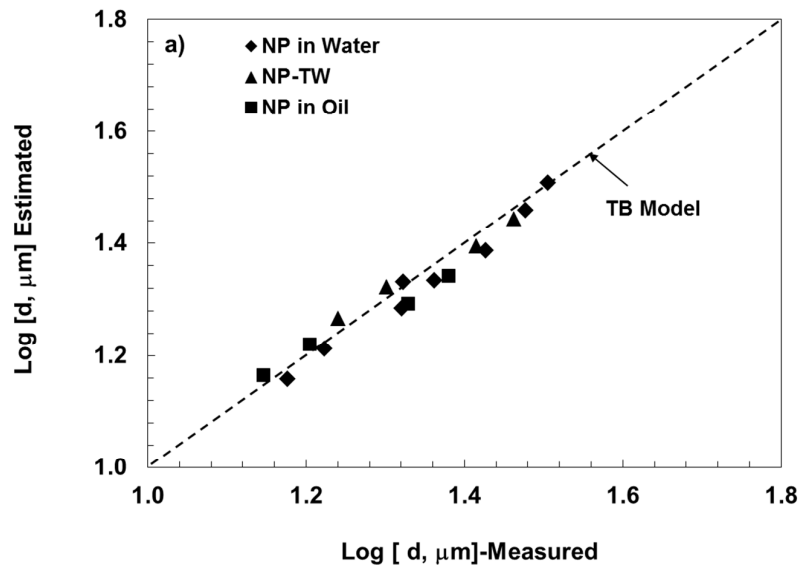
$$\left(\frac{3}{2} \right) k_s \pi \tau d^2 \left(\frac{d}{2} \right) = \pi d_p \gamma \left(\frac{d_p}{2} \right) \quad (11)$$

Defining the dimensionless droplet size $\xi = d/d_p$, Eq. (11) reads,

$$\left(\frac{3}{2} \right) k_s \xi^3 d_p^3 \tau = d_p^2 \gamma \quad (12)$$

Rearranging gives,

$$\xi = \sqrt[3]{\frac{2\gamma}{3k_s \tau d_p}} \quad (13)$$



Figs. 11a, 11b show comparison between measured droplet size and those predicted by the TB model for emulsions stabilized by ZIF-8 and MIL-101 NPs respectively.

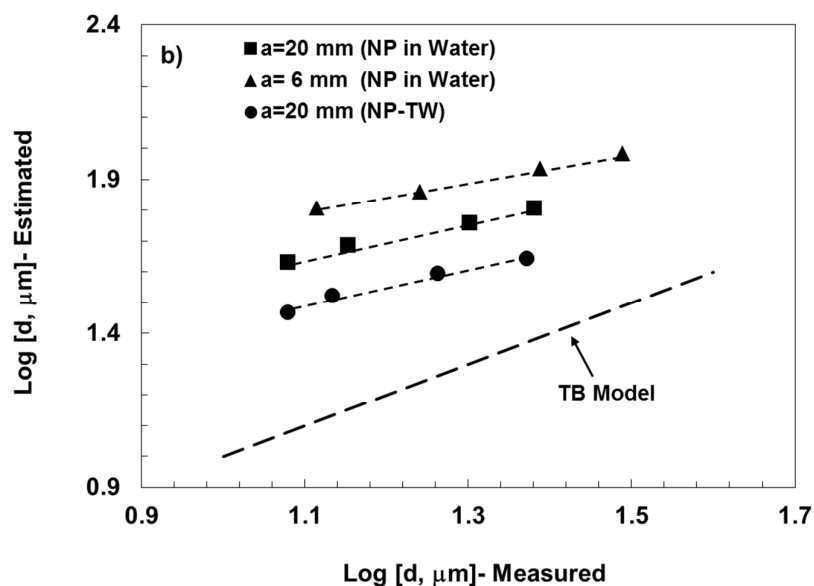


Figure 11. Comparison between measured drop size and predicted by TB model for emulsion stabilized by a) ZIF-8 NPs, b) MIL-101 NPs

As can be seen, the former gives good fit to the model predictions, while the latter deviates significantly. As discussed above, the simple TB model considers only the forces acting on a droplet during its formation until detachment, assuming the system interfacial properties remain unchanged throughout this time span. Accordingly, the model will fail to predict the average droplet size if the system interfacial characteristics change during such period due to for example, desorption of the stabilizing particles. Under these conditions, other mechanisms such as droplet breakage and/or coalescence may be triggered by the system hydrodynamics, which would result in changing the final emulsion average droplet size. We believe this to be the likely cause for the deviation of the TB model predictions for emulsions stabilized by MIL-101 NPs, which is less hydrophobic than ZIF-8 with lower affinity to the interface, and would be easier to detach from a droplet surface under the influence of the surrounding hydrodynamic forces leading to formation of larger droplets. Such droplets will have higher tendency for breakage to smaller satellite ones, particularly at higher oscillation intensities, and even possible coalescence of the formed satellite droplets into larger ones. This would result in significant changes to the originally formed emulsion droplets that cannot be predicted by simple TB analysis and is currently being investigated by our group.

CONCLUSIONS

This investigation demonstrate the possibly of successfully preparing Pickering emulsions stabilized by MIL-101 and ZIF-8 metal organic frameworks nanoparticles both in presence and absence of surfactants using a novel design oscillatory woven metal microscreen (WMMS) emulsification system. The results showed that, both the system hydrodynamics of and the hydrophobic/ hydrophilic nature of the NPs influenced the interfacial properties of the oil-water interface during droplet formation and after detachment which affected the final droplet size and distribution. The strong hydrophobic nature of ZIF-8 NPs resulted in higher affinity to surface, and formation of smaller and more stable droplets that resisted further breakage at high oscillations intensities. MIL-101 NPs on the other hand and due to its weaker hydrophobic nature resulted in formation of lager and less stable droplets with more tendency for breakage into smaller satellite droplets, particularly at intense oscillations. Such difference was also noticed when using surfactants, where synergy was observed with MIL-101 in both droplet size and stability through interfacial tension reduction and possible larger surface coverage. Compared to ZIF-8, larger droplets and wider distribution was observed, likely due to surfactant interaction with the NP, which resulted in decreasing surface coverage, and increasing the interfacial tensions.

List of Figures:

Figure 1: Crystal Structure of a) ZIF-8 and b) MIL-101

Figure 2: SEM of a) ZIF-8 and b) MIL-101

Figure 3: The Oscillatory Woven Metal Micro Screen (WMMS) apparatus

Figure 4: a) Microscopic image and b) droplet size distribution of the forming emulsions.

Figure 5: Stability of the formed emulsions over six months.

Figure 6. Variation of droplet size and distributions for emulsions stabilized using ZIF-8. Effect of: a) frequency, b) amplitude, c) dispersed phase flux.

Figure 7. Comparison between emulsions prepared using ZIF-8 in oil and water. Effect of oscillation frequency on a) droplet size, b) size distribution (CV)

Figure 8. Characteristics of emulsions stabilized using MIL-101. Effect of oscillation frequency on: a) droplet size, b) size distribution (CV)

Figure 9. Emulsions stabilized with MIL-101 in presence of Tween-20 surfactant. Effect of oscillation frequency on a) droplet size, b) size distribution (CV)

Figure 10. Emulsions stabilized with ZIF-8 in presence of Tween-20 surfactant. Effect of oscillation frequency on a) droplet size, b) size distribution (CV).

Figure 11. Comparison between measured drop size and predicted by TB model for emulsion stabilized by a) ZIF-8 NPs, b) MIL-101 NPs

List of Tables:

Table 1 : Physical properties of the systems

Nomenclature

- A oscillation amplitude (m).
 A interfacial area (m^2)
 CV coefficient of variation (%)
 D average droplet size (m).
 d_p pore diameter (m).
 E_d : desorption energy required to remove one NP from the interface (J)
 ΔE change in interfacial energy (J)
 f oscillation frequency (Hz)
 F_d shear force(N)
 F_s interfacial tension holding force (N)
 J Dispersed phase flux ($\text{m}^3 \cdot \text{m}^{-2} \cdot \text{h}^{-1}$)
 k_s wall correction factor (-).
 N number of droplets (-).
 N_p number of NPs in a given interfacial area A (-)
 R NP radius (m).
 t time (s)
 u continuous phase velocity at the droplet centre (ms^{-1}).
 y distance from the surface (m)
 γ interfacial tension (Nm^{-1}).
 η dimensionless distance from the surface (-)
 δ_s Stokes layer thickness (m)
 θ particle contact angle with the oil-water interface (Rad)
 ν_c continuous phase kinematic viscosity (m^2s^{-1}).
 ρ continuous phase density (kgm^{-3})
 τ shear stress (Pa)
 ξ dimensionless droplet size (-)
 ω angular frequency (s^{-1})

REFERENCES

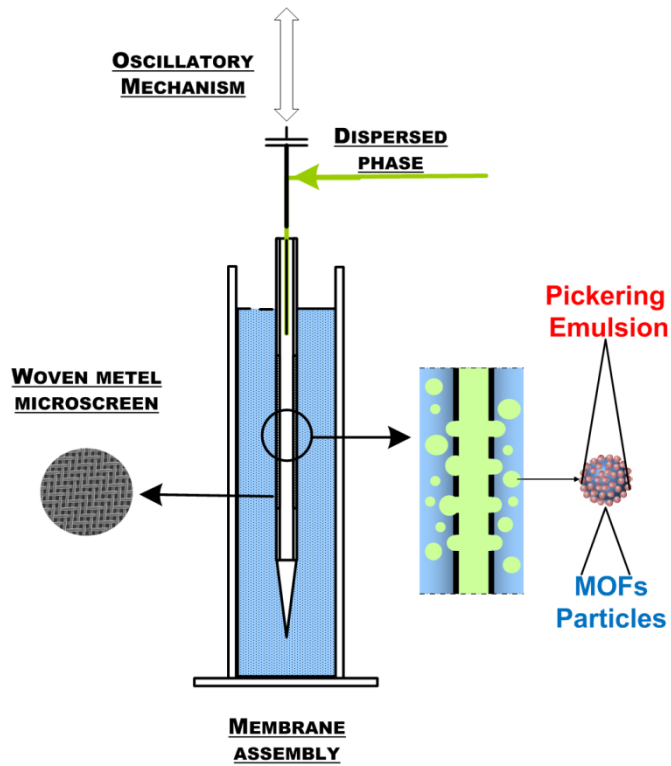
1. T. Welss, D. A. Basketter and K. R. Schröder, *Toxicology in Vitro*, 2004, 18, 231-243.
2. R. Aveyard, B. P. Binks and J. H. Clint, *Advances in Colloid and Interface Science*, 2003, 100–102, 503-546.
3. S. Jiang, Q. Chen, M. Tripathy, E. Luijten, K. S. Schweizer and S. Granick, *Advanced Materials*, 2010, 22, 1060-1071.
4. Y. Chevalier and M.-A. Bolzinger, *Colloids and Surfaces A: Physicochemical and Engineering Aspects*, 2013, 439, 23-34.
5. Y. He, *Materials Letters*, 2005, 59, 114-117.
6. J. Li and H. D. H. Stöver, *Langmuir*, 2010, 26, 15554-15560.
7. B. P. Binks and S. O. Lumsdon, *Langmuir*, 2000, 16, 2539-2547.
8. T. A. L. Do, J. R. Mitchell, B. Wolf and J. Vieira, *Reactive and Functional Polymers*, 2010, 70, 856-862.
9. S. U. Pickering, *Journal of the Chemical Society, Transactions*, 1907, 91, 2001-2021.
10. B. P. Binks and S. O. Lumsdon, *Langmuir*, 2001, 17, 4540-4547.
11. J. R. Long and O. M. Yaghi, *Chemical Society Reviews*, 2009, 38, 1213-1214.
12. Q. Yuan, O. J. Cayre, M. Manga, R. A. Williams and S. Biggs, *Soft Matter*, 2010, 6, 1580-1588.
13. G. T. Vladislavljević and R. A. Williams, *Advances in Colloid and Interface Science*, 2005, 113, 1-20.
14. A. J. Gijsbertsen-Abrahamse, A. van der Padt and R. M. Boom, *Journal of Membrane Science*, 2004, 230, 149-159.
15. E. Haque, N. A. Khan, J. H. Park and S. H. Jung, *Chemistry – A European Journal*, 2010, 16, 1046-1052.
16. J. Lee, O. K. Farha, J. Roberts, K. A. Scheidt, S. T. Nguyen and J. T. Hupp, *Chemical Society Reviews*, 2009, 38, 1450-1459.
17. S. Bourrelly, P. L. Llewellyn, C. Serre, F. Millange, T. Loiseau and G. Férey, *Journal of the American Chemical Society*, 2005, 127, 13519-13521.
18. H. G. Gomaa, J. Liu, R. Sabouni and J. Zhu, *Chemical Engineering Science*, 2014, 117, 161-172.
19. H. G. Gomaa, J. Liu, R. Sabouni and J. Zhu, *Colloids and Surfaces A: Physicochemical and Engineering Aspects*, 2014, 456, 160-168.

20. W. Zeng, H. G. Gomma, J. Liu and J. Zhu, *Chemical Engineering and Processing: Process Intensification*, 2013, **73**, 111-118.
21. G. T. Vladislavjević and R. A. Williams, *Journal of Colloid and Interface Science*, 2006, **299**, 396-402.
22. V. Schadler and E. J. Windhab, *Desalination*, 2006, **189**, 130-135.
23. M. S. Manga, O. J. Cayre, R. A. Williams, S. Biggs and D. W. York, *Soft Matter*, 2012, **8**, 1532-1538.
24. N. Aryanti, R. Hou and R. A. Williams, *Journal of Membrane Science*, 2009, **326**, 9-18.
25. J. Zhu and D. Barrow, *Journal of Membrane Science*, 2005, **261**, 136-144.
26. R. G. Holdich, M. M. Dragosavac, G. T. Vladislavjević and S. R. Kosvintsev, *Industrial & Engineering Chemistry Research*, 2010, **49**, 3810-3817.
27. E. Egidi, G. Gasparini, R. G. Holdich, G. T. Vladislavjević and S. R. Kosvintsev, *Journal of Membrane Science*, 2008, **323**, 414-420.
28. K. L. Thompson, S. P. Armes and D. W. York, *Langmuir*, 2011, **27**, 2357-2363.
29. K. S. Park, Z. Ni, A. P. Côté, J. Y. Choi, R. Huang, F. J. Uribe-Romo, H. K. Chae, M. O’Keeffe and O. M. Yaghi, *Proceedings of the National Academy of Sciences*, 2006, **103**, 10186-10191.
30. K. M. L. Taylor-Pashow, J. D. Rocca, Z. Xie, S. Tran and W. Lin, *Journal of the American Chemical Society*, 2009, **131**, 14261-14263.
31. R. Ananthoji, J. F. Eubank, F. Nouar, H. Mouttaki, M. Eddaoudi and J. P. Harmon, *Journal of Materials Chemistry*, 2011, **21**, 9587-9594.
32. I. B. Vasconcelos, T. G. d. Silva, G. C. G. Militao, T. A. Soares, N. M. Rodrigues, M. O. Rodrigues, N. B. d. Costa, R. O. Freire and S. A. Junior, *RSC Advances*, 2012, **2**, 9437-9442.
33. C.Y. Sun, C. Qin, X.-L. Wang, G.-S. Yang, K.-Z. Shao, Y.-Q. Lan, Z.-M. Su, P. Huang, C.-G. Wang and E.-B. Wang, *Dalton Transactions*, 2012, **41**, 6906-6909.
34. K. M. L. Taylor-Pashow, J. D. Rocca, Z. Xie, S. Tran and W. Lin, *Journal of the American Chemical Society*, 2009, **131**, 14261-14263.
35. P. Horcajada, T. Chalati, C. Serre, B. Gillet, C. Sebrie, T. Baati, J. F. Eubank, D. Heurtaux, P. Clayette, C. Kreuz, J.-S. Chang, Y. K. Hwang, V. Marsaud, P.-N. Bories, L. Cynober, S. Gil, G. Ferey, P. Couvreur and R. Gref, *Nat Mater*, 2010, **9**, 172-178.
36. M. Hartmann and M. Fischer, *Microporous and Mesoporous Materials*, 2012, **164**, 38-43.

37. G. Férey, C. Mellot-Draznieks, C. Serre, F. Millange, J. Dutour, S. Surblé and I. Margiolaki, *Science*, 2005, 309, 2040-2042.
38. S. Cao, T. D. Bennett, D. A. Keen, A. L. Goodwin and A. K. Cheetham, *Chemical Communications*, 2012, 48, 7805-7807.
39. H. Fan and A. Striolo, *Physical Review E*, 2012, 86, 051610.
40. C. P. Whitby, D. Fornasiero and J. Ralston, *Journal of Colloid and Interface Science*, 2008, 323, 410-419.
41. H. Nciri, N. Huang, V. Rosilio, M. Trabelsi-Ayadi, M. Benna-Zayani and J.-L. Grossiord, *Rheologica Acta*, 2010, 49, 961-969.
42. F. Ravera, M. Ferrari, L. Liggieri, G. Loglio, E. Santini and A. Zanobini, *Colloids and Surfaces A: Physicochemical and Engineering Aspects*, 2008, 323, 99-108.
43. Q. Lan, F. Yang, S. Zhang, S. Liu, J. Xu and D. Sun, *Colloids and Surfaces A: Physicochemical and Engineering Aspects*, 2007, 302, 126-135.
44. H. Ma, M. Luo and L. L. Dai, *Physical Chemistry Chemical Physics*, 2008, 10, 2207-2213.
45. F. Ravera, E. Santini, G. Loglio, M. Ferrari and L. Liggieri, *The Journal of Physical Chemistry B*, 2006, 110, 19543-19551.
46. C. Vashisth, C. P. Whitby, D. Fornasiero and J. Ralston, *Journal of Colloid and Interface Science*, 2010, 349, 537-543.
47. B.P. Binks, A. Desforges, D.G. Duff, Synergistic stabilization of emulsions by a mixture of surface-active nanoparticles and surfactant, *Langmuir* 23 (2007) 1098–1106
48. A. J. Goldman, R. G. Cox and H. Brenner, *Chemical Engineering Science*, 1967, 22, 653-660.
49. H. Schlichting, *Boundary-Layer Theory*, seventh ed., McGraw-Hill Book, Company, New York, 1979, p. 93.
50. S. R. Kosvintsev, G. Gasparini, R. G. Holdich, I.W. Cumming, M.T. Stillwell, Liquid-Liquid Membrane Dispersion in a Stirred Cell with and without Controlled Shear, *Ind. Eng. Chem. Res.* 44 (2005) 9323-9330.

Acknowledgement: The authors are grateful for the Natural Sciences and Engineering Research Council of Canada for the financial support. Grant # 238635-2012.

Table of content entry



Surfactant free Pickering emulsion was prepared using metal organic frameworks as stabilizers by Oscillatory Woven Metal Micro-Screen (WMMS).